Phenylene Vinylene Oligomers Studied by Theoretical Methods: Joint Analysis of Computational and X-Ray Results of the Configurational Isomers of 1,4-bis[2-(3,4,5-Trimethoxyphenyl) Ethenyl]Benzene

GUANG WU, S. JACOBS, M. G. VERBRUGGEN, A. T. H. LENSTRA, C. VAN ALSENOY, and H. J. GEISE*

University of Antwerpen (UIA), Department of Chemistry, Universiteitsplein 1, B-2610 Wilrijk, Belgium

L. VAN MEERVELT

Laboratory of Macromolecular Structural Chemistry, Catholic University of Leuven, Celestijnenlaan 200F, B-3001 Heverlee, Belgium

Received 15 June 1995; accepted 5 October 1995

ABSTRACT

The configurational isomers of 1,4-bis[2-(3,4,5-trimethoxyphenyl)ethenyl]benzene have been investigated by *ab initio* and MOPAC-AM1 semiempirical methods. The calculations were guided by and compared with single crystal X-ray results of the *trans, trans*-isomer (taken from the literature) and of the *cis,cis*-isomer (reported here). Using 4-21G-based *ab initio* calculations, free state geometries, deviations from coplanarity, and barriers to rotation of the central and peripheral rings were evaluated. Such barriers were also enumerated for the solid state of the *cis,cis*- and *trans,trans*-isomers. A single-molecule cluster surrounded by point charges sufficed to rationalize observed solid state properties in the *trans,trans*-isomer, including the quasi-free rotation of the central ring. A multimolecule cluster, however, was required to rationalize the restricted rotation of the rings in the *cis,cis*-isomer. MOPAC-AM1 methods were used to

*Author to whom all correspondence should be addressed.

Journal of Computational Chemistry, Vol. 17, No. 10, 1245–1257 (1996)

CCC 0192-8651 / 96 / 101245-13

calculate geometries and energies of rotameric forms on the singlet photoisomerization path *cis,cis* → *cis,trans* → *trans,trans*. Finally, UV absorption wavelengths and oscillator strengths were calculated and the electronic structure of the states discussed.

Introduction

Fully π-conjugated electro-optically active compounds have been the subject of extensive physical characterization, aimed chiefly at understanding the unique electrical, electrochemical, and optical properties of these materials. Among them, substituted phenylene vinylene oligomers, such as the title compound, 1,4-bis[2-(3,4,5-trimethoxyphenyl)ethenyl]benzene (henceforth abbreviated as TEB; see Fig. 1), are presently under investigation for use in organic light emitting devices (OLEDs)[1] and conductimetric sensors.[2]

TEB and similar trimers can be separated into the three configurational isomeric forms, that is, in the Z,Z- or *cis,cis*-, the Z,E- or *cis,trans*-, and the E,E- or *trans,trans*-configuration (abbreviated as c,c-TEB, c,t-TEB, and t,t-TEB, respectively). They differ significantly in spectroscopic and material properties.[3,4] Because detailed geometrical knowledge is a prerequisite for molecular engineering,[5-7] the aim of the present work is to study by *ab initio* and other theoretical methods: (i) the geometry of the most interesting conformation of each isomer; (ii) the deviation from planarity; (iii) the differences in ring rotational movements of the molecules in the free state and in the solid state; and (iv) the relation between these structural features and physical properties, such as solubilities, UV-Vis spectra, and isomerization processes. We will compare the sometimes explicitly mix the *ab initio* results with those obtained from NMR spectroscopy,[3] and from single crystal X-ray diffraction measurements. The latter data are partly taken from the literature[8] and partly from new determinations and presented here. In fact, the large number of possible conformations per isomer and their small expected energy differences drive us to the experiments for information about the most interesting forms. Moreover, the relevance of the computed rotational barriers becomes clear from the comparison of similarities and differences found in the X-ray structures.

Experimental

TEB was prepared by the Wittig reaction and the three configurational isomers were separated by high-pressure liquid chromatography (HPLC) using procedures described before.[3] To grow a single crystal, the solution of the *cis,cis*-isomer in chloroform was kept in the dark at −15°C to avoid photochemical isomerization into the *trans,trans*-isomer. After a few weeks, pale yellow, platelike crystals were obtained by slow evaporation of the

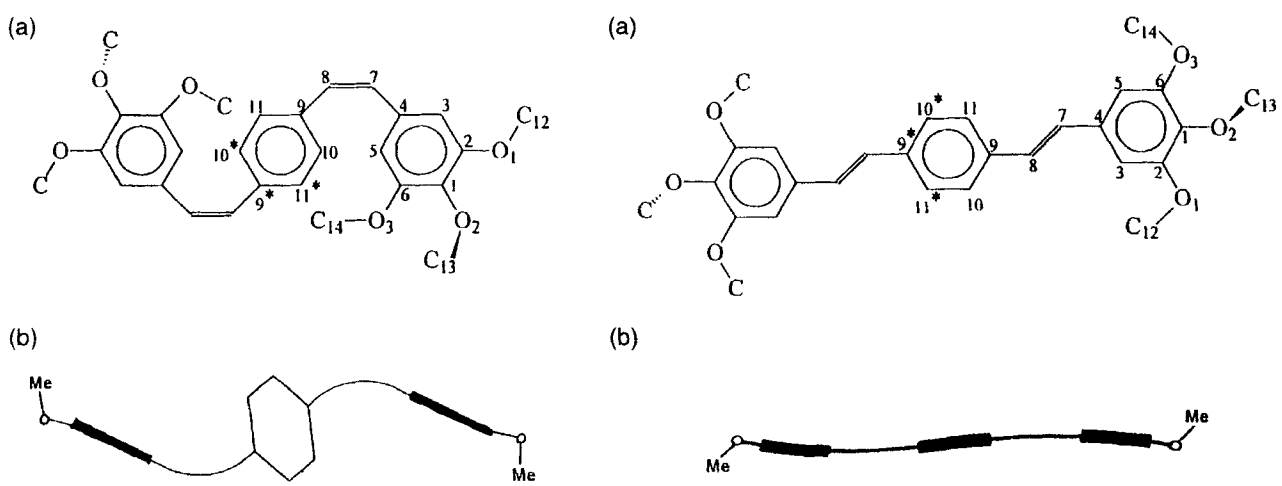

FIGURE 1. (a) Top view of structural formula and atomic numbering scheme of c,c-TEB (left) and t,t-TEB (right). (b) Side views of these molecules showing deviations from planarity (phenyl rings are shaded).

solvent. A crystal of size 0.4 × 0.25 × 0.25 mm was used for the structure determination. The determination of the cell dimensions and the data collection were performed on a Siemens P4-PC diffractometer with graphite monochromatized Cu-K_α radiation (λ = 1.54178 Å). Unit-cell parameters were determined from 20 reflections in the range 10° < 2θ < 28°. The data collection was performed at 16°C in the $\omega/2\theta$ scan mode with the scan angle set at 1.2°. Three intensity-control reflections were monitored every hour; no intensity decay was found. The space group $P2_1/c$, with half a molecule in the asymmetric unit, was inferred from systematic extinctions. The structure was solved using direct methods, after which all hydrogen atoms were defined from difference Fourier maps. Full-matrix least-squares refinements (on F^2) were carried out for all positional parameters with anisotropic temperature parameters for nonhydrogen atoms and isotropic temperature parameters for hydrogen atoms. Atomic scattering factors were taken from *International Tables for X-ray Crystallography*,[9] and the structure determination was performed using the program package SHELXL-93.[10] Crystallographic and least-squares refinement data are summarized in Table I. Final atomic positions and thermal parameters are given in Table II, while geometrical features are shown in Table III. The atomic numbering scheme used is illustrated in Figure 1. The crystal packing is shown in Figure 3.

TABLE I.
Crystallographic and Least-Squares Refinement Data of c,c-TEB.

Formula	$C_{28}H_{30}O_6$
M_w	462.52
Space group	$P2_1/c$; $Z = 2$
a (Å)	17.547(3)
b (Å)	7.645(2)
c (Å)	9.321(2)
β (°)	101.96(1)
V (Å^3)	1223.2(5)
D (X-ray) (g / cm^3)	1.256
F (000)	492
λ (Cu-K_α) (Å)	1.54178
μ (mm^{-1})	0.713
Data collection range	$5 < 2\theta < 101°$ $-17 \le h \le 17$ $-7 \le k \le 1$ $-1 \le l \le 9$
Number of data collected	1869
Number of unique reflections	1275
Number of data in refinement	1275
Number of variables	203
R [over reflections with $F > 4\sigma^2(F)$]	0.043
R_w[a] (over all reflections)	0.125
S	0.95
Δ/σ(max)	0.02
Highest peak in ΔFourier (e / Å^3)	0.17

[a] R_w defined as $R_w = \{\Sigma w(F_{obs}^2 - F_{calc}^2)^2 / \Sigma w(F_{obs}^2)^2\}^{1/2}$ with $w = 1 / \{\sigma^2(F_{obs}^2) + (0.1045P)^2 + 0.03P\}$ and $P = \{\max(F_{obs}^2, 0) + 2F_{calc}^2\} / 3$.

Computational Methods

The Hartree–Fock gradient[11,12] geometry optimizations using the 4-21G[12] basis set were performed using the program package, BRABO,[13,14] which is the version for large molecules of the TEXAS program[15] by Pulay. Free state structures of the three configurations of TEB were optimized without any constraints. The geometries were refined with the standard convergence criterion[16]; i.e., until the largest residual force on any atom is less than 0.001 mdyn. The optimized conformations with relevant torsion angles are shown in Figure 2a–c, and the numerical geometry parameters are summarized in Table III. The atomic numbering used in the remainder of this work is given in Figure 1 and Table II; note the difference from the IUPAC numbering.

Next, we enumerated the rotational barriers when rotating the outer ring around C(4)—C(7), and when rotating the central ring around C(8)—C(9), respectively. Since we are only seeking a semiquantitative insight into the free state rotational properties, we changed only the relevant torsion angle in these calculations, and did not optimize any of the other geometrical parameters. Figure 4 gives the rotational barriers of the *cis,cis*- and of the *trans,trans*-isomer with reference to the C(5)—C(4)—C(7)—C(8) torsion angle for the outer ring (φ1) and to the C(7)—C(8)—C(9)—C(10) torsion angle for the central ring (φ2).

To obtain the corresponding information about geometry and rotational properties in the solid state the crystal field cluster approach was followed.[17–20] In its simplest form the model (so-called PC model) contains *one* central molecule described by a wave function (single molecule ψ-moiety). The ψ-moiety is surrounded by point charges put at atomic positions generated in accordance with the space group symmetry of the material. In the case of c,c-TEB, the ψ-moiety is sur-

TABLE II.

Positional Parameters in Fractions of the Cell Edges, Equivalent Isotropic Temperature Parameters (Å²), and a Selection of Short Intermolecular Contacts (Å).[a]

Atom	x	y	z	B_{iso} (Å²)
O(1)	0.5789(1)	−0.0739(2)	0.1374(2)	4.58(8)
O(2)	0.5928(1)	0.1855(2)	0.3293(2)	4.74(8)
O(3)	0.7257(1)	0.2350(2)	0.5303(2)	5.61(8)
C(1)	0.6542(1)	0.0710(3)	0.3371(1)	3.55(8)
C(2)	0.6465(1)	−0.0707(3)	0.2421(2)	3.47(8)
C(3)	0.7045(1)	−0.1976(3)	0.2571(3)	3.55(8)
C(4)	0.7716(1)	−0.1824(3)	0.3674(2)	3.55(8)
C(5)	0.7799(1)	−0.0384(3)	0.4607(3)	3.87(8)
C(6)	0.7219(1)	0.0883(3)	0.4447(2)	3.79(8)
C(7)	0.8298(2)	−0.3233(3)	0.3861(3)	4.74(8)
C(8)	0.9067(2)	−0.3128(4)	0.4336(3)	5.21(8)
C(9)	0.9545(1)	−0.1532(3)	0.4670(3)	4.11(8)
C(10)	1.0077(1)	−0.1347(4)	0.6004(3)	4.58(8)
C(11)	0.9488(1)	−0.0161(4)	0.3676(3)	4.50(8)
C(12)	0.5679(2)	−0.2126(4)	0.0327(4)	5.21(8)
C(13)	0.6018(2)	0.3522(4)	0.2666(5)	5.92(8)
C(14)	0.7971(2)	0.2766(5)	0.6239(3)	5.37(8)
H(3)	0.6987(2)	−0.293(3)	0.194(2)	4.0(5)
H(5)	0.826(1)	−0.0263(4)	0.537(2)	4.1(5)
H(7)	0.8094(6)	−0.440(3)	0.3595(8)	5.4(6)
H(8)	0.9335(9)	−0.419(4)	0.4476(6)	6.7(7)
H(10)	1.0143(2)	−0.232(3)	0.674(2)	5.5(6)
H(11)	0.914(1)	−0.0263(5)	0.275(3)	4.9(6)
H(12,1)	0.521(2)	−0.183(3)	−0.043(3)	5.7(6)
H(12,2)	0.565(2)	−0.330(4)	0.081(3)	6.2(7)
H(12,3)	0.614(2)	−0.214(4)	−0.025(4)	8.2(8)
H(13,1)	0.551(2)	0.408(4)	0.264(3)	6.9(7)
H(13,2)	0.611(2)	0.341(5)	0.173(5)	10(1)
H(13,3)	0.648(2)	0.411(5)	0.338(4)	9.5(9)
H(14,1)	0.789(2)	0.394(4)	0.664(3)	7.0(7)
H(14,2)	0.840(2)	0.281(4)	0.564(3)	6.6(7)
H(14,3)	0.817(2)	0.184(5)	0.702(4)	9.1(9)

Atom in mol. at x,y,z[b]	Atom in Mol. 2[c]	Distance (Å)	Mol. 2 at:
O(3)	C(13D)	3.466	$x, -1/2-y, -1/2+z$
C(11)	C(14B)	3.618	$x, -1/2-y, -3/2+z$
C(6)	C(14B)	3.658	$x, -1/2-y, -3/2+z$
O(3)	C(1D)	3.666	$x, -1/2-y, -1/2+z$
C(2)	C(12A)	3.679	$x, -3/2-y, -1/2+z$
O(3)	C(2D)	3.682	$x, -1/2-y, -1/2+z$
C(1)	C(14B)	3.695	$x, -1/2-y, -3/2+z$
C(1)	C(12A)	3.778	$x, -3/2-y, -1/2+z$

[a] The esd's given in parentheses refer to the last significant digit. See Figure 1 for atomic numbering scheme. H(*i*,*j*) designates H atom *j* attached to C(*i*). Equivalent isotropic temperature parameters were calculated from anisotropic temperature parameters using $B(\text{iso}) = 4/3[a^2B(1,1) + b^2B(2,2) + c^2B(3,3) + ab(\cos\gamma)B(1,2) + ac(\cos\beta)B(1,3) + bc(\cos\alpha)B(2,3)]$.

[b] Numbering scheme is defined in Figure 1.

[c] Molecules A,B,D refer to Figure 5.

TABLE III.
Geometrical Parameters of TEB Isomers.[a]

Bond parameter	trans,trans Crystal[b] C_i	trans,trans Free (*ab initio*) C_i	cis,cis Crystal C_i	cis,cis Free (*ab initio*) C_i	cis,trans Free (*ab initio*)[c] C_1
O(1)—C(2)	1.371(3)	1.378	1.370(3)	1.378	1.379 (1.378)
O(1)—C(12)	1.430(3)	1.442	1.427(3)	1.441	1.442 (1.445)
O(2)—C(1)	1.376(2)	1.384	1.379(3)	1.385	1.384 (1.385)
O(2)—C(13)	1.419(3)	1.458	1.424(4)	1.459	1.459 (1.459)
O(3)—C(6)	1.363(3)	1.378	1.370(3)	1.380	1.377 (1.380)
O(3)—C(14)	1.439(3)	1.442	1.406(3)	1.445	1.442 (1.445)
C(1)—C(2)	1.392(2)	1.389	1.388(3)	1.388	1.389 (1.388)
C(1)—C(6)	1.384(3)	1.385	1.393(3)	1.387	1.385 (1.387)
C(2)—C(3)	1.384(3)	1.381	1.392(3)	1.384	1.381 (1.384)
C(3)—C(4)	1.396(3)	1.391	1.397(3)	1.389	1.391 (1.389)
C(4)—C(5)	1.395(3)	1.389	1.391(3)	1.387	1.389 (1.387)
C(4)—C(7)	1.474(3)	1.479	1.469(3)	1.487	1.479 (1.487)
C(5)—C(6)	1.393(3)	1.384	1.391(3)	1.382	1.384 (1.382)
C(7)—C(8)	1.315(3)	1.324	1.333(4)	1.324	1.324 (1.324)
C(8)—C(9)	1.465(3)	1.477	1.477(4)	1.487	1.478 (1.486)
C(9)—C(10)	1.364(3)	1.394	1.398(3)	1.392	1.393 (1.390)
C(9)—C(11)	1.368(3)	1.393	1.388(4)	1.391	1.393 (1.393)
C(10)—C(11*)	1.379(3)	1.378	1.382(4)	1.381	1.379 (1.380)
C(2)—O(1)—C(12)	117.3(4)	120.3	118.3(2)	120.2	120.3 (120.2)
C(1)—O(2)—C(13)	114.9(4)	115.5	116.0(2)	115.7	115.6 (115.8)
C(6)—O(3)—C(14)	118.1(4)	120.3	118.5(2)	119.7	120.2 (119.7)
O(2)—C(1)—C(2)	119.3(4)	120.4	119.3(2)	120.0	120.6 (120.0)
O(2)—C(1)—C(6)	121.3(4)	120.4	121.2(2)	120.8	120.3 (120.8)
C(2)—C(1)—C(6)	119.4(4)	119.2	119.4(2)	119.2	119.1 (119.2)
O(1)—C(2)—C(1)	114.8(4)	115.3	115.1(2)	115.8	115.3 (115.8)
O(1)—C(2)—C(3)	124.1(4)	124.0	124.5(2)	124.0	123.9 (123.9)
C(1)—C(2)—C(3)	121.2(4)	120.7	120.4(2)	120.2	120.8 (120.3)
C(2)—C(3)—C(4)	119.5(4)	120.1	120.2(2)	120.3	120.1 (120.3)
C(3)—C(4)—C(5)	119.6(4)	119.1	119.2(2)	119.5	119.1 (119.5)
C(3)—C(4)—C(7)	122.2(4)	123.0	119.0(2)	118.8	123.0 (118.8)
C(5)—C(4)—C(7)	118.0(4)	117.9	121.7(2)	121.6	117.9 (121.6)
C(4)—C(5)—C(6)	120.2(4)	120.6	120.3(2)	120.0	120.6 (120.0)
O(3)—C(6)—C(1)	115.5(4)	115.7	115.4(2)	115.7	115.8 (115.8)
O(3)—C(6)—C(5)	124.2(4)	124.0	124.2(2)	123.6	123.9 (123.5)
C(1)—C(6)—C(5)	120.3(4)	120.3	120.4(2)	120.7	120.3 (120.7)
C(4)—C(7)—C(8)	127.4(5)	126.7	128.8(2)	128.7	126.7 (128.8)
C(7)—C(8)—C(9)	126.6(5)	126.7	127.6(2)	128.9	126.6 (128.9)
C(8)—C(9)—C(10)	120.7(5)	118.7	121.1(2)	119.3	118.6 (119.4)
C(8)—C(9)—C(11)	123.8(4)	123.8	121.6(2)	122.3	123.6 (122.4)
C(10)—C(9)—C(11)	115.4(4)	117.5	117.4(2)	118.3	117.8 (118.1)
C(9)—C(10)—C(11*)	122.6(5)	121.6	120.9(2)	121.1	121.5 (121.3)
C(9)—C(11)—C(10*)	122.1(5)	120.9	121.7(2)	120.6	120.8 (120.6)
C(12)—O(1)—C(2)—C(1)	174.4(4)	171.4	−178.0(2)	−172.3	170.5 (−172.2)
C(12)—O(1)—C(2)—C(3)	−5.7(5)	−9.5	2.4(3)	8.1	−10.5 (8.1)
C(13)—O(2)—C(1)—C(2)	106.9(4)	89.6	106.8(3)	−101.2	84.2 (−101.8)
C(13)—O(2)—C(1)—C(6)	−77.3(4)	−91.8	−77.5(3)	80.1	−97.1 (79.7)
C(14)—O(3)—C(6)—C(1)	177.5(4)	−171.2	169.4(2)	166.3	−170.5 (165.2)
C(14)—O(3)—C(6)—C(5)	−3.7(5)	9.7	−11.0(4)	−14.7	10.2 (−15.7)
C(4)—C(7)—C(8)—C(9)	171.0(4)	180.0	6.2(5)	4.6	−179.7 (4.6)
C(8)—C(7)—C(4)—C(3)	6.8(6)	1.4	−149.2(3)	−141.9	3.6 (−142.5)
C(8)—C(7)—C(4)—C(5)	−168.6(4)	−179.1	33.7(4)	41.0	−177.0 (40.3)
C(7)—C(8)—C(9)—C(10)	177.9(4)	180.0	−129.3(3)	−139.1	174.8 (−139.3)
C(7)—C(8)—C(9)—C(11)	−5.6(6)	0.0	51.0(4)	43.3	−5.7 (43.5)

[a]Lengths are given in angstroms, and angles are given in degrees. The esd's given in parentheses refer to last significant digit.
[b]From ref. 8.
[c]Data in parentheses represent the parameters related to the cis portion.

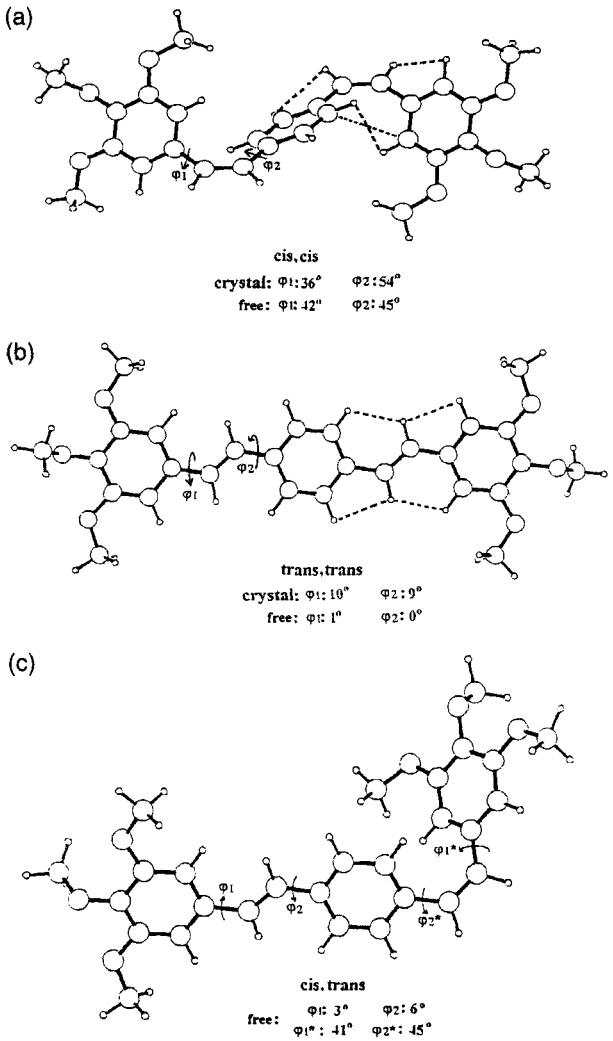

FIGURE 2. Geometries of TEB isomers: (a) *cis,cis*-configuration; (b) *trans,trans*-configuration; and (c) *cis,trans*-configuration. Reference torsion angle φ_1 = C(5)—C(4)—C(7)—C(8), and torsion angle φ_2 = C(7)—C(8)—C(9)—C(10).

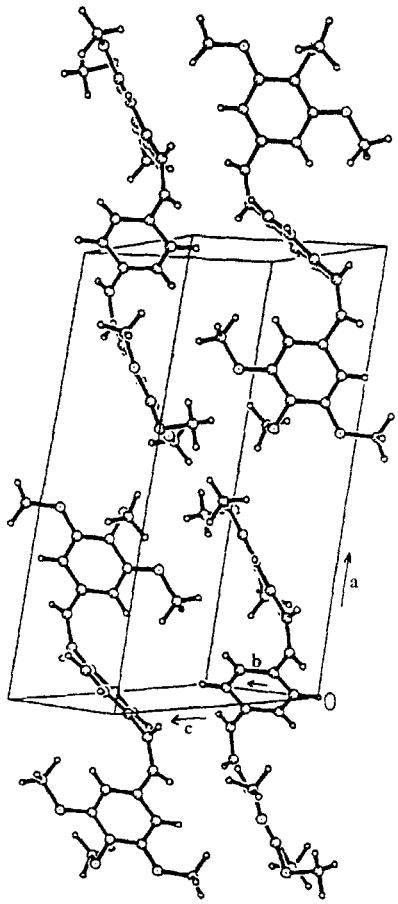

FIGURE 3. View of the crystal packing of the *cis,cis* isomer of TEB.

rounded in a zone of 15-Å thickness by 6528 point charges put on positions generated by the $P2_1/c$ space group symmetry and having charge values obtained in a Mulliken analysis.[21] The approach is computationally simple, and recent methodological improvements[22,23] have made it successful in reproducing the crystalline state geometry of a number of organic molecules.[17,22-26] However, here the purpose is not to reproduce the solid state geometry, but rather to investigate the solid state effect upon material properties. Therefore, we did not optimize the geometry of the ψ-moiety in the solid state calculations. Instead, we kept the ψ-moiety fixed to the geometry observed in the X-ray determination.

The PC model works well for weak intermolecular interactions. In some cases, however, including c,c-TEB, intermolecular interactions cannot be treated solely electrostatistically, and one has to treat a cluster of molecules quantum-mechanically. Then, the single molecule ψ-moiety is replaced by a multimolecule ψ-moiety, again surrounded by an envelope of point charges (so-called SM model). Unfortunately, for c,c-TEB, even a modest five-molecule ψ-moiety would require a wave function containing 320 (C, H, O) atoms and 1830 contracted Gaussian basis sets. This is outside the limits of the program BRABO,[27,28] which allows up to about 200 atoms and 1500 basis functions. As a compromise, we constructed the multimolecule ψ-moiety shown in Figure 5. It consists essentially of the asymmetric unit of c,c-TEB (i.e., half a TEB molecule of point symmetry C_i) and one outer ring of the four crystallographically nearest

molecules as deduced from Figure 3. The ψ-moiety now contains 139 (C, H, O) atoms and 770 contracted Gaussian functions. Since this choice makes it impossible to perform a meaningful Mulliken charge calculation, we did not surround the ψ-moiety by point charges. The barrier to rotation around C(4)—C(7) was then calculated rotating the outer ring E (see Fig. 5) while keeping the other atoms in the ψ-moiety fixed. A justification of the approach will be supplied *a posteriori* by the result given in Figure 4.

Finally, taking the *ab initio* ground state as reference, we calculated wavelengths and oscillator strengths of the electronic transitions for the three TEB isomers, as well as their excitation energies and the energies of the two transition states between them on the singlet photoisomerisation path c,c-TEB → c,t-TEB → t,t-TEB. These computations were performed using the semiempirical program package MOPAC[29] in the AMI approach.[30]

In the calculations, configurational interactions were included using an active space of six orbitals consisting of two groups of orbitals closely spaced in energy, i.e., the occupied orbitals HOMO through HOMO-3 and the unoccupied orbitals LUMO and LUMO + 1.

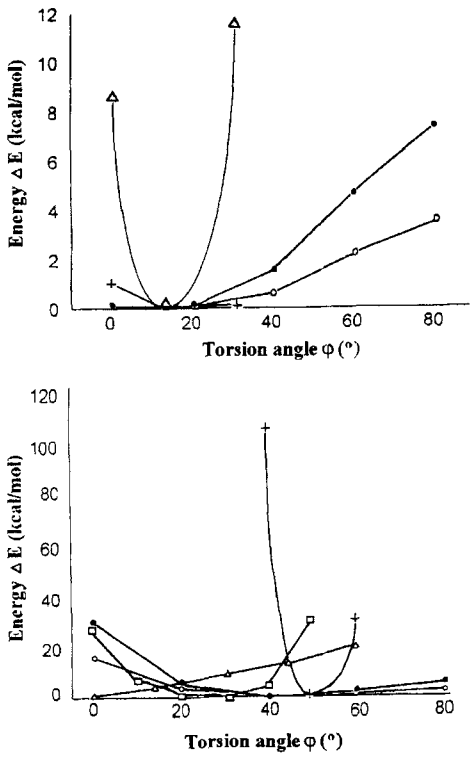

FIGURE 4. *Ab initio* calculated rotational barriers in the free and in the solid state of *cis,cis*-TEB (lower) and *trans,trans*-TEB (upper). (•) Free state central ring; reference torsion angle C(7)—C(8)—C(9)—C(10). (+) Solid state central ring; reference torsion angle C(7)—C(8)—C(9)—C(10). (○) Free state outer ring; reference torsion angle C(5)—C(4)—C(7)—C(8). (△) Solid state outer ring; reference torsion angle C(5)—C(4)—C(7)—C(8). (□) Solid state outer ring; reference torsion angle C(5)—C(4)—C(7)—C(8). Calculated using "multimolecule Ψ-moiety" (see text).

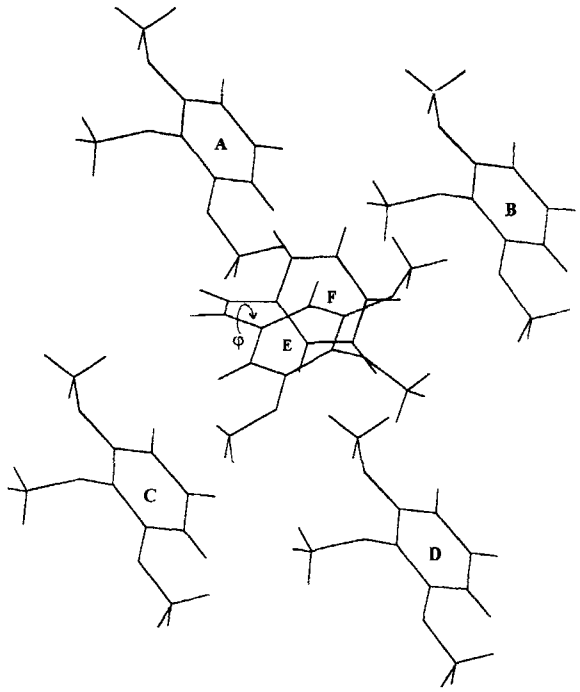

FIGURE 5. Molecular fragments used as multimolecule Ψ-moiety in SM model of the solid state of *cis,cis*-TEB.

Results and Discussion

CRYSTAL STRUCTURES

As indicated in the Introduction we start by discussing the similarities and dissimiliarities observed in the X-ray structures, and note (see Fig. 1) that both t,t-TEB and c,c-TEB have C_i symmetry in the crystalline state. From the comparison of geometries (Table III) and of thermal parameters (Table II and Table I of ref. 8) the following features can be extracted.

First, the most notable dissimilarity concerns the differences in the coplanarities of individual planar moieties. For example (see Fig. 2), in t,t-TEB the least-squares planes of the outer and central phenyl ring deviate from the ethenylene plane by $\varphi_1 = 10°$ and $\varphi_2 = 9°$, respectively, while the two

phenyl rings include a dihedral angle of 14°. Such relatively small dihedral angles are probably dictated by crystal packing requirements, because the *ab initio* calculations indicate that the free state molecule has a shallow potential well around the equilibrium geometry $\varphi_1 = \varphi_2 = 0°$ (Fig. 4).

In the *cis,cis*-isomer, however, the planar moieties show much more serious deviations from coplanarity. The outer and central phenyl rings deviate from the ethenylene plane by $\varphi_1 = 36°$ and $\varphi_2 = 54°$. In c,c-TEB, the packing may have only a minor effect; the deviations from coplanarity are now dictated by intramolecular steric hindrance, because the *ab initio* calculations show (Fig. 4) similar distortions from coplanarity for the free state molecule. Very similar phenomena were observed in electron diffraction studies of gaseous *trans*- and *cis*-stilbene[31,32] and in two other *cis*-phenylene ethenylene oligomers.[33]

Second, in both isomers the methoxy groups O(1)—C(12) and O(3)—C(14) are almost coplanar with the outer phenyl ring, whereas the middle methoxy group O(2)—C(13) is almost perpendicular to the ring. The bond lengths and valence angles associated with these OCH_3 groups are very similar in both isomers. They also closely follow the calculated values as well as values calculated for the ortho- and eclipsed conformations of anisole.[34,35]

Third, the distributions of bond lengths and valence angles experimentally found in the phenylene ethenylene backbones of both isomers are again very similar. Moreover, they agree rather well with the values calculated for the free state molecules. The only exceptions are the O(3)—C(14) length in c,c-TEB and the C(9)—C(10) and C(9)—C(11) lengths in t,t-TEB, all of which are too short as a result of large amplitude torsion movement. The observation for the latter two bond lengths is of particular interest for the subsequent discussion of differences in rotational freedom. In c,c-TEB, the average CC bond lengths in the outer (1.392 Å) and central ring (1.391 Å) are normal, and thus support the conclusion that the shrinkage of C(9)—C(10) and C(9)—C(11) in t,t-TEB is the result of large amplitude motion.

This, together with the observed sequences of atomic thermal parameters (outer phenyl ring < ethenylene link < O atoms < Me atoms < central phenyl ring for t,t-TEB,[8] compared to outer phenyl ring < central phenyl ring < ethenylene link < O atoms < Me atoms for c,c-TEB; (Table II), proves that only the central ring in t,t-TEB exhibits large amplitude motion, whereas none of the rings in c,c-TEB shows any sign of such motion.

Fourth, the crystal packing shows (Table II and Fig. 3) that short intermolecular contacts in c,c-TEB occur between methoxy atoms and atoms of the outer as well as the central rings. This rationalizes the absence of large amplitude motion in c,c-TEB. In contrast, the packing of t,t-TEB (Table 2 in ref. 8) only shows short intermolecular contacts between mutual methoxy groups and between methoxy atoms and ethenylene atoms. This rationalizes the occurrence of central ring motion (see also next section).

Furthermore, the range of short contacts in c,c-TEB is from 3.4 to 3.8 Å and in t,t-TEB from 3.3 to 3.5 Å. The more irregularly shaped and more loosely packed c,c-TEB is, as might be expected, more soluble and has a lower melting point than t,t-TEB.

The X-ray results may be summarized as proof of: (i) small, but distinct differences in intermolecular contacts; (ii) considerably different coplanarities; and (iii) large amplitude motion in the central ring of t,t-TEB. Consequently, inter- as well as intramolecular interactions play an important role in deciding the rotational freedom of a particular ring. Therefore, extensive investigations of energies, geometries, and rotational barriers may lead to an understanding of structure–property relations.

AB INITIO OPTIMIZED GEOMETRIES AND ROTATIONAL BARRIERS

We recall that, with the exception of some torsion angles and parameters related to the central ring of t,t-TEB, the 4-21G optimized geometries (r_e-type) of t,t-TEB and c,c-TEB are consistent with those from the X-ray analyses. The deviations of bond lengths and valence angles, described as $\Sigma|r(\text{X-ray})\text{-}r(\text{4-21G})|/\Sigma r(\text{X-ray})$, are 7.7×10^{-3} and 6.6×10^{-3} for the t,t-isomer, and 7.7×10^{-3} and 4.9×10^{-3} for the c,c-isomer. The agreement is as good as can be expected, keeping in mind that 4-21G calculated CO distances and COC angles are generally overestimated,[36] and that one compares free state r_e-geometries with solid state r_α^0-geometries.[22]

Turning to t,t-TEB, the optimized free state geometry (Table III, Fig. 2) has C_i symmetry, and is planar allowing complete π-conjugation. Nevertheless, the rotation barriers of the outer and central rings (Fig. 4) indicate broad energy minima; i.e., ring rotation over 50° from the equilibrium $\varphi = 0°$

takes less than 3.5 kcal mol^{-1}. In other words, the rings have rotational freedom over an angle as large as about 100°. Ring rotation leads to a decrease in steric hindrance between H atoms (Fig. 2) as well as to a decrease in resonance stabilization. Hence, the shallow potentials are the result of two competing effects. Indeed, an electron diffraction study of the similar molecule, *trans*-stilbene, in the gas phase gave[31] an averaged dihedral angle of 33° between the phenyl ring and the ethenyl plane.

Moreover, the NMR spectra of t,t-TEB in solution show[37] the same chemical shifts for the atom pairs H(3)/H(5), H(10)/H(11), C(3)/C(5), and C(10)/C(11), also indicating the rotational freedom of the phenyl rings.

The softness of the intramolecular rotations suggests that the dihedral angles in the solid state may be dictated by packing effects and may be rather different from those in the free state. It follows from the solid state calculations at the level of the PC model (Fig. 4) that the potential well of the outer ring is shifted to $\phi_1 = 10°$ and is significantly narrowed due to dense intermolecular contacts. In contrast, the central ring rotation remains to show a shallow energy distribution, because there is still free space to accomodate the rotation of that ring. Taking the average r_e distance of 1.394 Å for C(9)—C(10) and C(9)—C(11) and 1.366 Å as the average observed r_α^0-distance, the rotation of the central ring may be estimated as $\arccos(1.366/1.394) = 11.5°$. Considering the observed value $\phi_2 = 9°$, the actual value may vary between roughly $\varphi_2 = -10°$ and $\varphi_2 = 40°$. Clearly, such a motion costs little energy in view of the potential distribution.

Next, we focus on c,c-TEB. The calculations indicate a free state molecule with a decidedly nonplanar structure and torsion angles φ_1 and φ_2 close to those in the solid state (Fig. 2). Also, the free state c,c-TEB geometry is consistent with the structure of *cis*-stilbene determined by gas phase electron diffraction.[32] Inspection of the calculated free state ring rotations shows (Fig. 2) both rings to have an asymmetric potential, which is somewhat steeper than in t,t-TEB.

The asymmetry arises because starting from, e.g., $\varphi_2 = 54°$, it makes a difference whether the central ring rotates toward a coplanar or toward a perpendicular orientation with respect to the ethenylene plane. Rotation toward coplanarity will raise the energy due to short C(5)...C(10) and H(5)...H(10) contacts. Rotation toward a perpendicular orientation will also increase the energy, but being caused by weakening π-electron conjugation in a different way. Similar arguments apply to the outer ring rotation. Hence, the calculations predict the rings in free state c,c-TEB to have somewhat less rotational freedom that those in t,t-TEB. Nevertheless, it will not show in the solution NMR spectra of these isomers. In fact the remaining freedom together with the nonplanar geometry eliminate the distinction between the C(10)H(10)/C(11)H(11) and C(3)H(3)/C(5)H(5) pairs in c,c-TEB, just as the quasi-free rotation does in t,t-TEB.

In the solid state, ring rotational movements normally decrease, and neither the outer nor the central ring of c,c-TEB exhibits large amplitude motion. Solid state calculations, using the PC model, correctly reproduce the potential minimum of the central ring [φ_2(calc) = 50° vs. φ_2(X-ray) = 54°], but perform poorly in reproducing the potential minimum of the outer ring [φ_1(calc) = 0° vs. φ_1(X-ray) = 36°]. The reason for this failure was sought in a covalent (Van der Waals) rather than an electrostatic character of the short contacts between the methoxy substituents on adjacent molecules. To overcome this deficiency we constructed an SM model, i.e., the multimolecule ψ-moiety discussed in the "Computational Methods" section. The approach proved successful. The potential minimum now agrees much better with the X-ray result [φ_1(calc) = 32° vs. φ_1(X-ray) = 36°] and the potential well became much steeper (see Fig. 4). The comparison between the SM potential and that of the free state identifies *intra*molecular interactions (hindrance) to dominate the energy increase when the outer ring rotates toward being parallel to the ethenyl plane, and identifies *inter*molecular interactions (Van der Waals) to dominate the energy increase when the ring rotates toward being perpendicular. The PC potential of the central ring being steeper than the SM potential of the outer ring does not agree with the X-ray sequence of thermal parameters [B(outer) < B(central)]. We believe that the PC potential is too steep, but the present computer facilities do not allow us to perform the SM-type calculations necessary for this situation.

Finally, the optimized structure of free state c,t-TEB shows features pertinent to c,c-TEB as well as to t,t-TEB. The NMR spectra of the c,t-isomer indeed show[37] signals similar to those of the two other isomers, but neither gas phase electron nor X-ray diffraction results are available.

ELECTRONIC STRUCTURES AND ISOMERIZATION

Wittig reactions with semistabilized ylids always yield mixtures of Z and E isomers.[38] In this case, the Wittig reaction at room temperature resulted in an almost statistical distribution with ratio c,c:c,t:t,t = 3:4:3. Also, under illumination, c,c-TEB and c,t-TEB easily transform into t,t-TEB. These observations suggest small energy differences between the isomers. The calculations gave (Table IV) an energy sequence consistent with the above in which the differences are less than 5.3 kcal/mol.

The HOMO-LUMO energy gaps, calculated by *ab initio* and MOPAC methods (Table IV) follow the same order as the total molecular energies. These energy parameters are all correlated to the amount of π-electron conjugation and thus to molecular planarity. From the obtained molecular geometries, these energy sequences can be easily understood.

As a preparation to further research into the mechanism of the photochemical processes, c,c-TEB → c,t-TEB → t,t-TEB, we used MOPAC to evaluate the singlet isomerization paths. We assumed two transition states to have an ethenylene plane perpendicular to the central ring.[39] The results, illustrated in Figure 6, show numerical values close to those found in similar compounds.[40] They also indicate the c,t → t,t step to be faster than the c,c → c,t step, which is indeed observed for TEB. Of course, it must be realized that the real process may be more complicated and that firm conclusions must await investigations into possible triplet isomerization pathways.[39,40]

Finally, wavelengths and oscillator strengths of electronic transitions have been calculated using the MOPAC program and the AM1 model,[30] which is reported[41] to give better transition energies than the PM3 model.[42]

The results are given in Table V. Although the observed λ_{max} occur at wavelengths about 40 nm longer than the calculated values, the configurational effect is well reproduced: each transconfiguration in the structure is accompanied by a bathochromic shift of about 20 nm.

We recall that, in the configurational approach to the UV energies, we included the four orbitals closest in energy to the HOMO, LUMO, i.e., we included the series (HOMO-3),...,(LUMO + 1). This renders the interpretation of the transition types more difficult, because the transitions now contain significant contributions from transitions between orbitals located below and above the HOMO/LUMO. Note that we disregard different spin states. Nevertheless, information can be extracted from the orbital pictures given in Figure 7, in conjunction with Table V.

First, the compounds c,c-TEB and t,t-TEB exhibit C_i symmetry and their orbitals (LUMO + 1), ,...,(HOMO-3) belong to the A_u and A_g symmetry species in an alternating sequence. Thus (HOMO-i) → LUMO transitions are only allowed for $i = 0, -2$, whereas (HOMO-i) → (LUMO + 1) transitions are limited to $i = -1, -3$. Such restrictions do not apply for the c,t-TEB isomer with C_1 symmetry, allowing six instead of three transitions in the 190–370-nm range.

Second, the mixing of n, π^*, and π, π^* transitions results from the nonplanarity of the molecules. Indeed, the smallest mixing occurs in t,t-TEB, the isomer the least deviating from planarity.

Also, *increased* mixing induces a *decreasing* oscillator strength, which explains the observed high intensity of the longest wavelength absorption in t,t-TEB.

Third, mixing increases *inter alia* with a decreasing energy difference between the states. This explains why the (HOMO-1) → LUMO and HOMO → (LUMO + 1) transitions in c,t-TEB (forbidden in the other isomers) so strongly mix.

Fourth, the longest wavelength absorption (at $\lambda \approx 320$ nm) of all isomers is due to the HOMO →

TABLE IV.
Calculated Energy Parameters for the TEB Isomers.

	ΔE_{total} (kcal/mol)		E_{HOMO} (eV)		E_{LUMO} (eV)	
Isomer	*Ab initio*	MOPAC	*Ab initio*	MOPAC	*Ab initio*	MOPAC
cis,cis	5.18	6.39	−7.48	−8.71	2.55	−0.46
trans,trans	0.00	0.00	−7.05	−8.46	1.88	−0.89
cis,trans	2.45	2.74	−7.26	−8.62	2.21	−0.63

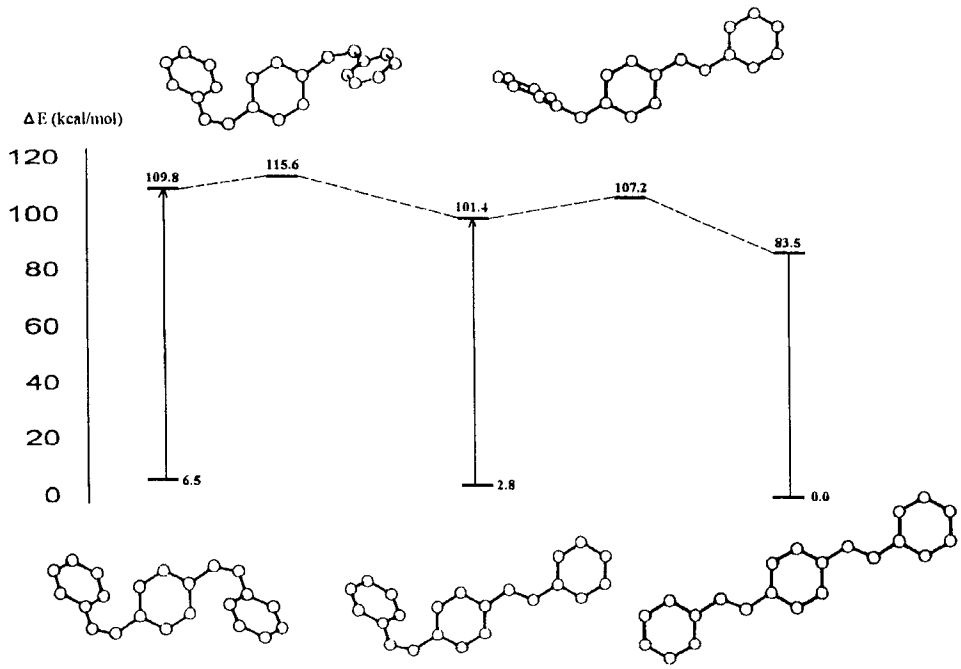

FIGURE 6. Calculated energies on the singlet isomerization path of TEB configurations.

TABLE V.
Observed Longest Wavelength Absorption (nm) and Calculated Wavelengths (nm) and Oscillator Strengths of Electronic Transition of TEB Isomers.

Configuration	Observed λ_{max} (nm)	λ_{calc} (nm)	Oscillator strength (relative unit)	Orbital excitation	Contribution (%)
cis,cis		286	9.36	HOMO → LUMO	74.8
				HOMO-1 → LUMO + 1	23.9
	330	249	5.12	HOMO-2 → LUMO	59.4
				HOMO-3 → LUMO + 1	39.2
		191	3.08	HOMO-1 → LUMO + 1	73.8
				HOMO → LUMO	24.1
trans,trans		321	19.15	HOMO → LUMO	81.7
				HOMO-1 → LUMO + 1	17.3
	368	255	4.57	HOMO-2 → LUMO	60.5
				HOMO-3 → LUMO + 1	33.6
		193	0.26	HOMO-1 → LUMO + 1	79.3
				HOMO → LUMO	17.4
cis,trans		297	8.83	HOMO → LUMO	78.4
				HOMO-1 → LUMO + 1	20.6
	353	260	5.97	HOMO-1 → LUMO	40.7
				HOMO → LUMO + 1	36.3
				HOMO-1 → LUMO + 1	11.0
		253	2.38	HOMO-2 → LUMO + 1	54.9
				HOMO-2 → LUMO	38.0
		246	2.83	HOMO-3 → LUMO	75.6
				HOMO-3 → LUMO + 1	21.1
		210	0.26	HOMO-1 → LUMO	41.0
				HOMO → LUMO + 1	40.1
		194	0.38	HOMO-1 → LUMO + 1	60.3
				HOMO → LUMO	15.1
				HOMO → LUMO + 1	13.5

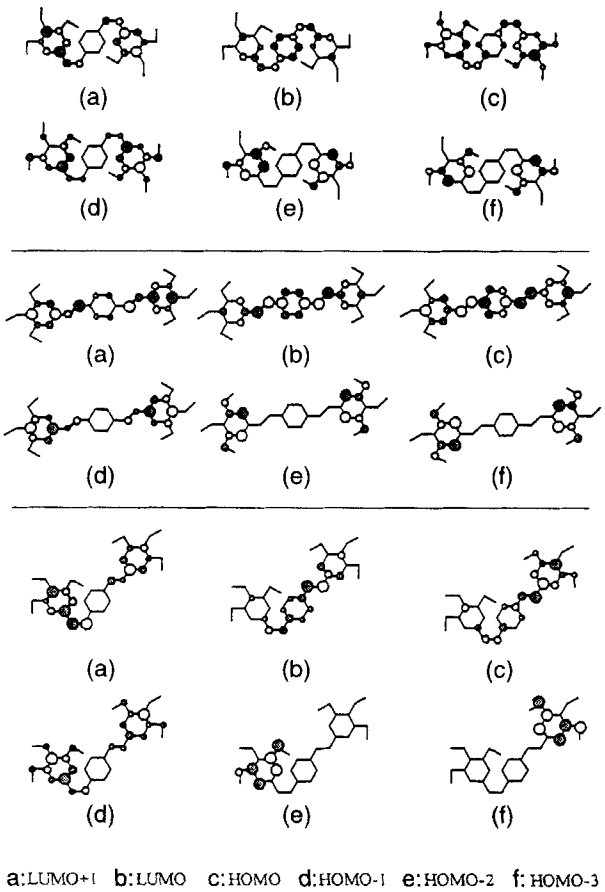

FIGURE 7. Orbital coefficients at atomic centers for the molecular orbitals involved in the electronic transitions of TEB. Orbital coefficients of opposite sign are displayed by open and filled circles. The radius of each circle is proportional to the orbital coefficient of the corresponding p_z-orbital population.

LUMO transition (ca. 75%) mixed with the (HOMO-1) → (LUMO + 1) transition (ca. 25%). Judged by the p_z-orbital occupancies we note that these transitions reflect a flow of electrons from the outer parts of the molecules (mostly from the phenyl rings when the HOMO is concerned, and mostly from the methoxy groups when the HOMO-1 is concerned) to the inner parts (most notably to the central ring when the LUMO is involved, and mostly to the double bonds when the LUMO + 1 is involved). Similar phenomena can be seen for the other absorption wavelengths. In other words, upon excitation these molecules acquire more polarity (quadrupolarity) by making the outer side more positive and the inner side more negative.

Acknowledgments

C. V. A., L. V. M., and M. G. V. thank the Belgian National Fund for Scientific Research, NFWO, for the appointments as senior research associates and as senior research assistant, respectively. Financial aid to the laboratory from the Flemish Ministry of Education (Contract Geconcerteerde Actie 89/94-10) is gratefully acknowledged. This text also presents research results of the Belgian Program on Interuniversity Attraction Poles, initiated by the Belgian State (Prime Minister's Office), Science Policy Programming. Scientific responsibility, however, is assumed by the authors.

Supplementary material available: Supplementary material containing a table of anisotropic displacement parameters and F_{obs}/F_{calc} listings are available from the authors upon request.

References

1. W. Tachelet, S. Jacobs, H. Ndayikengurukiye, H. J. Geise, and J. Grüner, *Appl. Phys. Lett.*, **64,** 2364 (1994).
2. M. De Wit, Ph.D. thesis, University of Antwerp (UIA) (forthcoming).
3. S. Jacobs, W. Eevers, G. Verreyt, H. J. Geise, A. De Groot, and R. Dommisse, *Synth. Met.*, **61,** 189 (1993).
4. Z. Yang and H. J. Geise, *Synth. Met.*, **47,** 95 (1992).
5. H. Eckhardt, L. W. Shacklette, K. Y. Jen, and R. L. Elsenbaumer, *J. Chem. Phys.*, **91,** 1303 (1989).
6. P. Brendel, A. Grupp, M. Mehring, R. Schenk, K. Mullen, and W. Huber, *Synth. Met.*, **45,** 49 (1991).
7. S. Zalis and M. Kertesz, *Synth. Met.*, **47,** 179 (1992).
8. M. Verbruggen, Y. Zhou, A. T. H. Lenstra, and H. J. Geise, *Acta Cryst.*, **C44,** 2120 (1988).
9. *International Tables for X-ray Crystallography*, vol. IV, The Kynoch Press, Birmingham, UK, 1974, Table 2.2B.
10. G. M. Sheldrick, SHELXL-93 (program for crystal structure refinement), University of Göttingen, Göttingen, Germany (1993).
11. P. Pulay, *Mol. Phys.*, **17,** 197 (1969).
12. P. Pulay, G. Fogarasi, F. Pang, and J. E. Boggs, *J. Am. Chem. Soc.*, **101,** 2550 (1979).
13. C. Van Alsenoy, *J. Comput. Chem.*, **9,** 620 (1988).
14. C. Van Alsenoy and A. Peeters, *J. Mol. Struct. (Theochem)*, **286,** 19 (1993).
15. P. Pulay, *Theor. Chim. Acta* **50,** 299 (1979).
16. L. Schäfer, *J. Mol. Struct.*, **100,** 51 (1983).
17. S. Saebo, B. Klewe, and S. Samdal, *Chem. Phys. Lett.*, **97,** 499 (1983).
18. J. G. Angyan, B. Silvi, *J. Chem. Phys.*, **86,** 6957 (1987).
19. J. Bridet, S. Fliszar, S. Odiot, and R. Pick, *Int. J. Quant. Chem.*, **24,** 687 (1983).

20. M. J. Mombourquette, J. A. Weil, and P. G. Mezey, *Can. J. Chem.*, **62,** 21 (1984).
21. R. S. Mulliken, *J. Chem. Phys.*, **23,** 1833, 2333, 2338 (1955).
22. P. Popelier, A. T. H. Lenstra, C. Van Alsenoy, and H. J. Geise, *Struct. Chem.*, **2,** 3 (1991).
23. P. Popelier, A. T. H. Lenstra, C. Van Alsenoy, and H. J. Geise, *Acta Chem. Scand. (Ser. A)*, **42,** 539 (1988).
24. T. U. Helgaker and B. Klewe, *Acta Chem. Scand. (Ser. A)* **42,** 269 (1988).
25. P. Popelier, A. T. H. Lenstra, C. Van Alsenoy, and H. J. Geise, *J. Am. Chem. Soc.*, **111,** 5658 (1989).
26. A. T. H. Lenstra, C. Van Alsenoy, K. Verhulst, and H. J. Geise, *Acta Cryst.*, **B50,** 96 (1994).
27. A. Peeters, C. Van Alsenoy, A. T. H. Lenstra, and H. J. Geise, *Int. J. Quant. Chem.*, **46,** 73 (1993).
28. A. Peeters, C. Van Alsenoy, A. T. H. Lenstra, and H. J. Geise, *J. Mol. Struct. (Theochem)*, **304,** 101 (1994).
29. J. J. Stewart, MOPAC, Program 455, Quantum Chemistry Program Exchange, University of Indiana, Bloomington, IN.
30. M. J. S. Dewar, E. G. Zoebisch, E. F. Healy, and J. J. P. Stewart, *J. Am. Chem. Soc.*, **107,** 3902 (1985).
31. M. Traetteberg, E. B. Frantsen, F. C. Mylhoff, and A. Hoekstra, *J. Mol. Struct.*, **26,** 57 (1975).
32. M. Traetteberg and E. B. Frantsen, *J. Mol. Struct.*, **26,** 69 (1975).
33. M. Hakansson, S. Jagner, M. Sundahl, and O. Wennerström, *Acta Chem. Scand.*, **46,** 1160 (1992).
34. D. C. Spellmeyer, P. D. J. Grootenhuis, M. D. Miller, L. F. Kuyper, and P. A. Kollman, *J. Phys. Chem.*, **94,** 4483 (1990).
35. V. A. Naumov, L. L. Tuzova, J. De Smedt, C. Van Alsenoy, and H. J. Geise, *J. Mol. Struct.*, **344,** 117 (1995).
36. L. Schäfer, C. Van Alsenoy, and J. N. Scarsdale, *J. Mol. Struct.*, **86,** 349 (1982).
37. S. Jacobs (unpublished results).
38. O. Wennerström, I. Raston, M. Sundahl, and D. Tanner, *Chem. Struct.*, **27,** 567 (1987).
39. K. Sandros, M. Sundahl, O. Wennerström, and U. Norinder, *J. Am. Chem. Soc.*, **112,** 3082 (1990).
40. M. Sundahl, O. Wennerström, K. Sandros, T. Arai, and K. Tokumaru, *J. Phys. Chem.*, **94,** 6731 (1990).
41. J. C. Panitz, T. Lippert, J. Stebani, O. Nuyken, and A. Wokaun, *J. Phys. Chem.*, **97,** 5246 (1993).
42. J. J. P. Stewart, *J. Comput. Chem.*, **10,** 209, 211 (1989).
43. J. J. P. Stewart, *J. Comput.-Aided Mol. Des.*, **4,** 1 (1990).